Letter

Multiple insulating states due to the interplay of strong correlations and lattice geometry in a single-orbital Hubbard model

H. L. Nourse, Ross H. McKenzie, and B. J. Powell
School of Mathematics and Physics, The University of Queensland, Brisbane, Queensland 4072, Australia

(Received 13 March 2020; revised 1 February 2021; accepted 8 February 2021; published 26 February 2021)

We report 10 ground states arising from strong correlations in the single-orbital Hubbard model on the decorated honeycomb lattice, including Dirac metals, flat-band ferromagnets, real-space Mott insulators, dimer and trimer Mott insulators, and a spin-1 Mott insulator. The rich phase diagram arises from structures within the unit cell. Hence, such states are absent on simpler lattices. We argue that such insulating phases are prevalent on decorated lattices. These are found in many materials and common in coordination polymers, providing a playground to explore this physics.

DOI: 10.1103/PhysRevB.103.L081114

Decorated lattices are found in a wide range of materials, including inorganic compounds [1–6], organometallics [7], organic molecular crystals [8], and coordination polymers (CPs) [9–18]. They consist of one or more cluster types, e.g., a molecule, linked to form a net [18,19]. Many materials with decorated lattices are reported to have novel ground states [20–33]. Perhaps the simplest is the decorated honeycomb lattice (DHL), realized in materials such as the trinuclear organometallic compounds, e.g., $Mo_3S_7(dmit)_3$ [7], in organic molecular crystals [8], in iron (III) acetates [1], in cold fermionic atoms [34], and in CPs [15–17]. There are a number of theoretical studies that predict exotic phases of matter on this lattice, such as the quantum spin Hall insulator [24], the quantum anomalous Hall insulator [25–27], topological metals [27], valence bond solids (VBS) [35–38], and quantum spin liquids [39–43] with non-Abelian anyons [39–41].

Rich phase diagrams often arise from the complex interplay of interactions between multiple orbitals, as found in the discovery and analysis of the superconducting pnictide compounds [44]. Here, we report a rich phase diagram with only a single orbital and an on-site Hubbard repulsion, but multiple sites in the unit cell. This suggests an alternative minimal path to rich physics arising from the unique structure of decorated lattices that is not found in simpler lattices.

In this Letter, we study the single-orbital Hubbard model on the DHL [Fig. 1(a)]. Despite the model having only three parameters (t_g/t_k, U/t_k, n), we find a plethora of interaction-driven phases (Table I). Some of the insulators occur away from half-filling where a metal is expected. These arise because of effective multiorbital interactions due to the structures that decorate the lattice. We construct simple pictures of these insulating phases by studying appropriate "molecular" limits—analogous to the atomic limit for the usual Mott-Hubbard transition. Low-energy effective theories of these insulators include the spin-1/2 Heisenberg model on the kagome lattice, and the spin-1/2 and spin-1 Heisenberg models on the honeycomb lattice (Figs. 1 and 2). We argue that such "molecular" Mott insulators are prevalent in decorated lattices. With the chemical flexibility found in CPs, decorated lattices provide an avenue to explore rich physics in condensed-matter systems.

The Hamiltonian for the Hubbard model on the DHL [7] is

$$\hat{H} \equiv -t_g \sum_{\langle i\alpha, j\alpha\rangle,\sigma} \hat{c}^{\dagger}_{i\alpha\sigma}\hat{c}_{j\alpha\sigma} - t_k \sum_{i,\alpha\neq\beta,\sigma} \hat{c}^{\dagger}_{i\alpha\sigma}\hat{c}_{i\beta\sigma} + U\sum_{i,\alpha}\hat{n}_{i\alpha\uparrow}\hat{n}_{i\alpha\downarrow}, \quad (1)$$

where $\hat{c}^{\dagger}_{i\alpha\sigma}$ ($\hat{c}_{i\alpha\sigma}$) creates (annihilates) an electron with spin $\sigma \in \{\uparrow, \downarrow\}$ on site $\alpha \in \{1, 2, 3\}$ of triangle cluster i, $\hat{n}_{i\alpha\sigma} \equiv \hat{c}^{\dagger}_{i\alpha\sigma}\hat{c}_{i\alpha\sigma}$, t_g (t_k) is the intertriangle (intratriangle) hopping integral [Fig. 1(a)], $\langle i\alpha, j\alpha\rangle$ signifies nearest-neighbor hopping between sites of adjacent triangles, and U is the local Coulomb repulsion.

We use rotationally invariant slave bosons (RISB) [45–48] to find the ground state of Eq. 1 using two-site [Figs. 2(a)–2(c)] or three-site clusters [Figs. 2(d)–2(f)], which are the minimal cluster sizes to capture the intracluster correlations necessary to describe the Mott insulators that we find away from half-filling in the kagome-like regime ($t_g/t_k > 3/2$) and the honeycomb-like regime ($t_g/t_k < 3/2$), respectively. Technical details can be found in the Supplemental Material [49]. Equivalent to the Gutzwiller approximation for multiorbital models [57], RISB renormalizes an uncorrelated wave function by adjusting the weights of local electronic configurations on a cluster, and at the mean-field level the metallic state is a simple realization of a Landau Fermi liquid. RISB successfully describes many strongly correlated phenomena [47,48,58–62]. The use of RISB allows us to capture important spatial correlations necessary for the insulators that we find, it describes exactly the limits of isolated trimers ($t_g = 0$) and isolated dimers ($t_k = 0$), and it allows us to study a wide range of parameters at a reasonable computational cost.

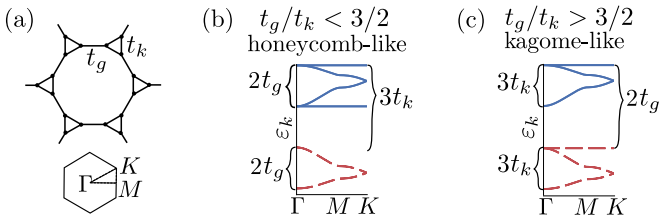

FIG. 1. (a) A triangle decorates each vertex of the honeycomb lattice. (b) Noninteracting band structure of the DHL with strong intratriangle hopping. The dashed (solid) line has mostly A (E) trimer orbital character [cf. Fig. 2(e)]. (c) Strong intertriangle hopping. The dashed (solid) line has mostly (anti)bonding orbital character [cf. Fig. 2(b)].

Insulators in RISB. Only the coherent part of the many-body Green's function matrix $\boldsymbol{G}(k,\omega)$ is captured within RISB. An effect of the correlations in the metallic state is a narrowing of the quasiparticle bands $\xi_p(k)$ (a band is indexed by p), and a loss of spectral weight, captured by the quasiparticle weight $Z_p^{\rm qp}(k)$ [49]. For quasiparticle bands that cross the Fermi energy ($\omega = 0$), RISB describes a Fermi liquid where $Z_p^{\rm qp}(k)$ is a measure of the metallicity, with $Z_p^{\rm qp}(k) = 1$ corresponding to a noninteracting metal and $Z_p^{\rm qp}(k) = 0$ to a correlated insulator, where the Fermi surface vanishes. This is the usual description of a Mott insulator at half-filling captured in slave boson theories [45], and originally described by Brinkman and Rice [63].

We work in the basis of the molecular orbitals (Fig. 2) where the quasiparticle weight is a diagonal matrix $\boldsymbol{Z}$, and we assume that the clusters are uniform. For two-site clusters $\boldsymbol{Z}_i = \mathrm{diag}(Z_b, Z_a)$ and for three-site clusters $\boldsymbol{Z}_i = \mathrm{diag}(Z_A, Z_{E_1}, Z_{E_2})$ with $Z_E \equiv Z_{E_1} = Z_{E_2}$. In the honeycomb-like regime [Fig. 1(b)], the lower (upper) bands have mostly A (E) orbital character, and in the kagome-like regime [Fig. 1(c)], the lower (upper) bands have mostly (anti)bonding orbital character. To a good approximation, the quasiparticle weight in the molecular orbital basis approximates the quasiparticle weight in the bands—they are exactly equivalent at the Γ and K points [49].

Real-space Mott insulator. The usual place to look for a Mott insulator is at half-filling ($n = 1$) because U disfavors double occupancy and suppresses charge fluctuations so that electrons become localized to a lattice site. For $t_g/t_k \leqslant 3/2$ and at finite U a metal-insulator transition occurs where the quasiparticle weight for all bands vanishes [Fig. 3(a)]. For $t_g/t_k > (t_g/t_k)_c = 0.9$–$1.0$, the dominating electronic configurations are spin-singlets along the t_g bonds [Fig. 4(b)], while for $t_g/t_k < (t_g/t_k)_c$ spin-singlets form along the t_k bonds. In the latter phase, there is an instability to a magnetic state that breaks the $\mathcal{C}_3$ rotational symmetry of the lattice [49].

The Heisenberg model on the DHL with exchange coupling $J_g = 4t_g^2/U$ and $J_k = 4t_k^2/U$ provides an effective model of the Hubbard model at large-U and $n = 1$. This model has been extensively studied [35–38]. Based on a detailed numerical study, it has been argued that for $J_g/J_k \gtrsim 0.9$ ($t_g/t_k \gtrsim 0.95$) a J_g-dimer VBS forms, while for $J_g/J_k \lesssim 0.9$ there is a VBS that favors spin-singlet formation along J_k bonds but breaks the $\mathcal{C}_3$ rotational symmetry of a triangle [38]. That our RISB calculations, which deal with the full fermionic degrees of freedom, qualitatively agree with calculations for the spin model (and give a good estimate for the critical coupling) suggests that RISB is a good approximation for the problem at hand.

TABLE I. Summary of the insulating states of the single-orbital Hubbard model on the decorated honeycomb lattice (DHL), where t_g (t_k) are the intertriangle (intratriangle) hopping amplitudes [Fig. 1(a)], and n is the filling per site. The ground-state candidates of the effective spin-$\mathcal{S}$ Heisenberg model in the Mott-insulating phases are in parentheses. QSL denotes quantum spin liquid and VBS denotes valence bond solid.

n	$t_g \lesssim t_k$	$\mathcal{S}$
1/3	Trimer Mott (honeycomb Néel order)	1/2
2/3	Band insulator	
5/6	Flatband ferromagnet	
1	Real-space Mott (broken $\mathcal{C}_3$ VBS)	1/2
4/3	Spin-1 Mott (honeycomb Néel order)	1
11/6	Flatband ferromagnet	
n	$t_g \gtrsim t_k$	$\mathcal{S}$
1/2	Dimer Mott (kagome QSL?)	1/2
5/6	Flatband ferromagnet	
1	t_g-dimer VBS (large U) crossover to band insulator (small U)	1/2
3/2	Dimer Mott (kagome QSL?)	1/2
11/6	Flatband ferromagnet	

Away from half-filling the naive expectation is a correlated metal because on average there is not one electron per site. However, the structure of the unit cell of decorated lattices provides important additional degrees of freedom that are not present in simpler lattices. Below we will show that these structures lead to several different interaction-driven insulators (Figs. 3 and 4), as is the case for multiorbital atomic systems.

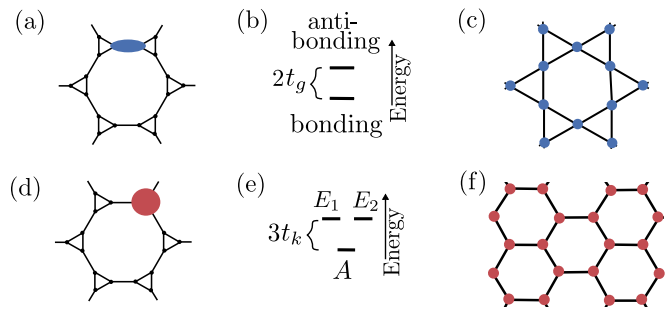

FIG. 2. Clusters used. (a) Clustering the DHL as dimers maps to a (b) two-orbital model on the (c) kagome lattice. (d) Clustering the lattice as trimers maps to an (e) three-orbital model on the (f) honeycomb lattice. In both cases there is complicated inter- and intraorbital hopping between clusters with phases that depend on direction.

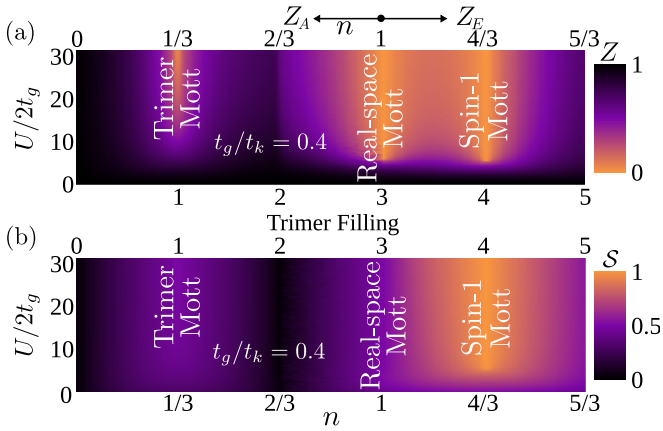

FIG. 3. Phase diagram in the honeycomb-like regime for the triangle clusters [Figs. 2(d)–2(f)]. (a) The relevant matrix element of $\boldsymbol{Z}$ that approximates the quasiparticle weight for bands at the Fermi energy. The quasiparticle weight vanishes in the Mott-insulating phases. For $n \leqslant 1$ ($n > 1$) we show the quasiparticle weight Z_A (Z_E) associated with the A (E) trimer orbital. At $n = 1$, $Z_A \sim Z_E$. (b) Effective spin $\mathcal{S}$ of a triangle, where $\mathcal{S}$ is the solution to $\mathcal{S}(\mathcal{S}+1) = \sum_i \langle \vec{S}_i \cdot \vec{S}_i \rangle / 2\mathcal{N}$, the spin of triangle i is $\vec{S}_i = \sum_{\alpha=1}^{3} \frac{1}{2} \sum_{\sigma\sigma'} \hat{c}^{\dagger}_{i\alpha\sigma} \vec{\tau}_{\sigma\sigma'} \hat{c}_{i\alpha\sigma'}$, $\vec{\tau}$ is a vector of Pauli matrices, and $\mathcal{N}$ is the number of unit cells. A spin-1/2 degree of freedom arises on each triangle in the real-space and trimer Mott insulators. A spin-1 moment occurs in the spin-1 Mott insulator because an effective intratriangle Hund's coupling $\tilde{J}$ favors the formation of spin-triplets on a triangle [64].

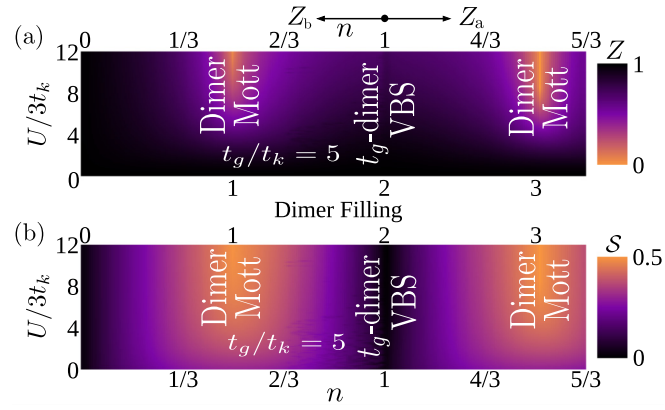

FIG. 4. Phase diagram in the kagome-like regime for the dimer clusters [Figs. 2(a)–2(c)]. (a) The relevant matrix element of $\boldsymbol{Z}$ that approximates the quasiparticle weight for bands at the Fermi energy. The quasiparticle weight vanishes in the Mott-insulating phases. For $n \leqslant 1$ ($n > 1$) we show the quasiparticle weight Z_b (Z_a) associated with the (anti)bonding dimer orbital. At $n = 1$, $Z_b \sim Z_a$. (b) Effective spin $\mathcal{S}$ of a dimer, where $\mathcal{S}(\mathcal{S}+1) = \sum_i \langle \vec{S}_i \cdot \vec{S}_i \rangle / 3\mathcal{N}$, and the spin of dimer i is $\vec{S}_i = \sum_{\alpha=1}^{2} \frac{1}{2} \sum_{\sigma\sigma'} \hat{c}^{\dagger}_{i\alpha\sigma} \vec{\tau}_{\sigma\sigma'} \hat{c}_{i\alpha\sigma'}$. A spin-1/2 degree of freedom arises on each dimer in the dimer Mott insulators. At half-filling, spin-singlet formation along the t_g bond leads to $\mathcal{S} = 0$.

Dimer Mott insulators. When intertriangle hopping is strong ($t_g/t_k > 3/2$), significant insight can be gained from working in the orbital basis of a dimer formed along the t_g bonds [Figs. 2(a)–2(c)]. The Hamiltonian describing a dimer has bonding and antibonding orbitals separated in energy by $2t_g$, with intraorbital and interorbital Coulomb repulsion ($\tilde{U} = U/2$), and interorbital spin-flip terms [49]. This leads to a model analogous to the Hubbard bilayer model [46] on the kagome lattice with complicated intersite hopping that mixes the bonding and antibonding orbitals.

In the dimer molecular limit ($t_g, U \to \infty$ with U/t_g finite), RISB with the cluster shown in Fig. 2(b) becomes exact. The mixing between the bonding and antibonding orbitals vanishes and the electronic structure contains two decoupled copies of the kagome lattice [Fig. 1(c)] with an intraorbital repulsion $\tilde{U}$. Half-filling the (anti)bonding orbital and turning on interactions is formally equivalent to the half-filled single-orbital Hubbard model on the kagome lattice [49]. A Mott insulator occurs for sufficiently large $\tilde{U}$ [65] and in the limit $\tilde{U} \to \infty$ is connected to the ground state of isolated dimers.

Our RISB results show that the dimer Mott insulators are extended phases away from these limits. In Fig. 4(a) we show the quasiparticle weight Z_b (Z_a) of the (anti)bonding orbitals for $n \leqslant 1$ (>1), which correspond to the lower (upper) bands in the kagome-like regime [Fig. 1(c)]. An insulator occurs at (three-)quarter-filling for sufficiently large U with the bonding orbitals half-filled (fully occupied) and the antibonding orbitals empty (half-filled). Interactions renormalize the electrons so that the dimer orbitals decouple, and the insulator is adiabatically connected to the insulator in the dimer molecular limit: a Mott insulator on the kagome lattice. As t_g/t_k is reduced, the dimer Mott insulator becomes unstable and there is instead a metal, occurring for $t_g/t_k \lesssim 4.1$ (3.0) for $n = 1/2$ (3/2).

The low-energy physics of the dimer Mott insulators is crucially different from the Mott insulator at half-filling. At half-filling the low-energy effective theory is the spin-1/2 Heisenberg model on the DHL. In the dimer Mott insulators, charge fluctuations are suppressed between dimers, with each dimer forming a spin $\mathcal{S} = 1/2$ moment [Fig. 4(b)]. Hence, the low-energy effective theory of the dimer Mott insulators is the spin-1/2 Heisenberg model on the kagome lattice, whose ground state may be a quantum spin liquid [66].

These dimer Mott insulators on the DHL are similar to those observed in the organic charge transfer salts κ-(BEDT-TTF)$_2X$, where the BEDT-TTF molecules form a dimer and share one hole [67–69]. For many X the intradimer hopping is more than twice the interdimer hopping [70], and a minimal model to describe the insulator is the half-filled single-orbital Hubbard model on the anisotropic triangular lattice [68,69]. Our results demonstrate that such insulators also arise in decorated lattices.

Trimer Mott insulator. The simplest way to understand the insulating phases in the limit of strong intratriangle hopping ($t_g/t_k < 3/2$) is to work in the eigenbasis of a triangle formed by the t_k bonds [Figs. 2(d)–2(f)]. The Hamiltonian describing a trimer has an A orbital separated in energy from two degenerate E orbitals by $3t_k$, with intraorbital and interorbital Coulomb repulsion $\tilde{U} = U/3$, a Hund's coupling $\tilde{J} = -\tilde{U}/3$ that favors spin-triplet formation on a triangle [21,22,64,71], interorbital spin-flip, and correlated interorbital hopping terms [49]. The Hamiltonian becomes a three-orbital model on the honeycomb lattice with complicated intersite hopping.

In the trimer molecular limit ($t_k, U \to \infty$, U/t_k finite), RISB with the cluster shown in Fig. 2(d) is exact. At one-sixth-filling ($n = 1/3$), the ground state has one electron in the A orbital with empty E orbitals. In this limit, the Hamiltonian is formally equivalent to the single-orbital Hubbard model on the honeycomb lattice [49]. A Mott insulator occurs for large $\tilde{U}$, and at $\tilde{U} \to \infty$ it is connected to the ground state of isolated trimers.

RISB demonstrates that the trimer Mott insulator is stable away from the trimer molecular limit, Fig. 3(a). However, for sufficiently small $\tilde{U}$, charge fluctuations between the A and E orbitals destroy the insulating state, and a Dirac metal is recovered. The trimer Mott insulator is adiabatically connected to the Mott insulator of the half-filled single-orbital Hubbard model on the honeycomb lattice. Hence, the low-energy effective theory is the spin-1/2 Heisenberg model on the honeycomb lattice whose ground state is Néel-ordered [72–79]. Above a critical hopping ratio $t_g/t_k \gtrsim 0.45$ the trimer Mott insulator is not found because a finite U is not sufficient to decouple the A and E orbitals and localize electrons.

Spin-1 Mott insulator. At two-thirds filling ($n = 2/3$), the trimer E orbitals are degenerate and the effective intraorbital interactions become crucial for understanding the insulating state. In the trimer molecular limit, RISB is exact and, for $U > 0$, the ground state contains a spin-triplet on each trimer due to the effective Hund's interaction $\tilde{J}$. For $t_k \gg t_g$ and $n > 1/3$, the Hamiltonian maps to a two-orbital Hubbard-Kanamori model on the honeycomb lattice with intersite hopping integrals whose phases are direction-dependent [49].

In Fig. 3(a) we show the quasiparticle weight Z_E of the E orbitals for $n > 1$, which corresponds to the upper bands in the honeycomb-like regime [Fig. 1(b)]. We find that Z_E vanishes, resulting in a metal-insulator transition from a Dirac metal to a spin-1 Mott insulator with the E (A) orbitals half-filled (fully occupied). In the insulator, the degenerate E orbitals are decoupled from the A orbitals with each triangle forming a spin-triplet because of the effective Hund's interaction $\tilde{J}$ [Fig. 3(b)]. Within RISB the spin-1 Mott insulator is adiabatically connected to the isolated trimer limit and a Mott insulator on the effective two-orbital model at half-filling on the honeycomb-like lattice. Above the critical hopping parameter ratio $t_g/t_k \gtrsim 0.86$ no spin-1 Mott insulator exists for finite U.

The low-energy effective theory of the spin-1 Mott insulator is the spin-1 Heisenberg model [43,80] on the honeycomb lattice whose ground state is Néel-ordered [81–84]. The molecular crystal $Mo_3S_7(dmit)_3$ is two-thirds filled, and an isolated monolayer is the DHL [7]. Hence, we propose that isolated monolayers of $Mo_3S_7(dmit)_3$ are spin-1 Néel-ordered.

Crucially, the spin-1 Mott insulator requires the effective Hund's coupling $\tilde{J}$ on a triangle. This can straightforwardly be confirmed by varying the effective multiorbital interactions. The dimer and trimer Mott insulators occur even when there is only an effective intraorbital Coulomb repulsion $\tilde{U}$ with no multiorbital interactions. In contrast, there is no Mott-insulating phase at two-thirds filling with only intraorbital $\tilde{U}$. A metal-insulator transition only occurs when the multiorbital interactions on a trimer are included.

Ferromagnetism. Mielke and Tasaki proved that the ground state of the Hubbard model with a flatband is a ferromagnetic insulator for $U > 0$ provided criteria are satisfied [85–87], which our model meets for any t_g/t_k and when the upper flatband is half-filled ($n = 11/6$). The criteria for the rigorous proof are not met by the lower flatband. Nevertheless, RISB predicts ferromagnetic long-range order when the lower flatband is partially filled ($2/3 < n < 1$) [49].

Additionally, the DHL has van Hove singularities at fillings $n = 1/4$, $5/12$, $5/4$, and $17/2$, where $\rho(E) \to \infty$. Due to the Stoner mechanism [88], the ground state is a ferromagnetic metal near $n = 1/4$ and $5/12$. However, antiferromagnetic correlations dominate near $n = 5/4$ and $17/2$ because of the proximity to the spin-1 Mott insulator [49].

Conclusions. Based on the above results, we propose that molecular Mott insulators are general on decorated lattices. The bases that diagonalize local structures within the unit cell of decorated lattices provide an intuitive picture of the insulating phases that are stabilized by strong electronic correlations. If the local structure is sufficiently complicated, then correlations can drive more exotic ground states, as demonstrated by the spin-1 Mott insulator at two-thirds filling on the DHL.

Many materials realize the DHL lattice [1,7,8,15–17,34]. Electronic structure calculations place some in the kagome-like [8,16] and others in the honeycomb-like [7,17] regimes. Several of these materials have insulating phases that have not previously had a detailed theoretical explanation. Chemical doping could allow for the exploration of their phase diagrams. More broadly, decorated lattices are common in CPs and found in many other classes of materials. These are typically insulating—but detailed theoretical explanations of these insulating states are largely absent. Our work provides the theoretical framework for understanding these materials.

An important open question is as follows: Do unconventional superconducting states generically arise near these molecular Mott-insulating phases? The superconductivity in the dimer Mott insulators in κ-(BEDT-TTF)$_2X$ [69,89,90] and some multiorbital models [23,91,92] and materials [44] suggest that they may.

Note added in proof. Near half-filling there is singlet superconductivity with extended-s, extended-d, and f-wave symmetry [93].

Acknowledgments. We thank Jason Pillay and Elise Kenny for helpful conversations. This work was supported by the Australian Research Council through Grants No. DP160102425, No. DP160100060, and No. DP181006201.

[1] Y.-Z. Zheng, M.-L. Tong, W. Xue, W.-X. Zhang, X.-M. Chen, F. Grandjean, and G. Long, Angew. Chem., Int. Ed. **46**, 6076 (2007).

[2] J.-K. Bao, J.-Y. Liu, C.-W. Ma, Z.-H. Meng, Z.-T. Tang, Y.-L. Sun, H.-F. Zhai, H. Jiang, H. Bai, C.-M. Feng, Z.-A. Xu, and G.-H. Cao, Phys. Rev. X **5**, 011013 (2015).

[3] L. T. Nguyen, T. Halloran, W. Xie, T. Kong, C. L. Broholm, and R. J. Cava, Phys. Rev. Mater. **2**, 054414 (2018).

[4] S. Taniguchi, T. Nishikawa, Y. Yasui, Y. Kobayashi, M. Sato, T. Nishioka, M. Kontani, and K. Sano, J. Phys. Soc. Jpn. **64**, 2758 (1995).

[5] F. Ye, S. Chi, W. Bao, X. F. Wang, J. J. Ying, X. H. Chen, H. D. Wang, C. H. Dong, and M. Fang, Phys. Rev. Lett. **107**, 137003 (2011).

[6] W. Bao, Q.-Z. Huang, G.-F. Chen, D.-M. Wang, J.-B. He, and Y.-M. Qiu, Chin. Phys. Lett. **28**, 086104 (2011).

[7] A. C. Jacko, C. Janani, K. Koepernik, and B. J. Powell, Phys. Rev. B **91**, 125140 (2015).

[8] Y. Shuku, A. Mizuno, R. Ushiroguchi, C. S. Hyun, Y. J. Ryu, B.-K. An, J. E. Kwon, S. Y. Park, M. Tsuchiizu, and K. Awaga, Chem. Commun. **54**, 3815 (2018).

[9] R. Murase, C. F. Leong, and D. M. D'Alessandro, Inorg. Chem. **56**, 14373 (2017).

[10] R. Murase, B. F. Abrahams, D. M. D'Alessandro, C. G. Davies, T. A. Hudson, G. N. L. Jameson, B. Moubaraki, K. S. Murray, R. Robson, and A. L. Sutton, Inorg. Chem. **56**, 9025 (2017).

[11] C. J. Kingsbury, B. F. Abrahams, D. M. D'Alessandro, T. A. Hudson, R. Murase, R. Robson, and K. F. White, Cryst. Growth Des. **17**, 1465 (2017).

[12] I.-R. Jeon, B. Negru, R. P. Van Duyne, and T. D. Harris, J. Am. Chem. Soc. **137**, 15699 (2015).

[13] L. E. Darago, M. L. Aubrey, C. J. Yu, M. I. Gonzalez, and J. R. Long, J. Am. Chem. Soc. **137**, 15703 (2015).

[14] J. A. DeGayner, I.-R. Jeon, L. Sun, M. Dincă, and T. D. Harris, J. Am. Chem. Soc. **139**, 4175 (2017).

[15] L. M. Henling and R. E. Marsh, Acta Crystallogr., Sect. C **70**, 834 (2014).

[16] K. M. Henline, C. Wang, R. D. Pike, J. C. Ahern, B. Sousa, H. H. Patterson, A. T. Kerr, and C. L. Cahill, Cryst. Growth Des. **14**, 1449 (2014).

[17] R. A. Polunin, V. N. Dorofeeva, A. E. Baranchikov, V. K. Ivanov, K. S. Gavrilenko, M. A. Kiskin, I. L. Eremenko, V. M. Novotortsev, and S. V. Kolotilov, Russ. J. Coord. Chem. **41**, 353 (2015).

[18] M. J. Kalmutzki, N. Hanikel, and O. M. Yaghi, Sci. Adv. **4** (2018).

[19] A. F. Wells, *Three-dimensional Nets and Polyhedra* (Wiley, New York, 1977).

[20] K. Ueda, H. Kontani, M. Sigrist, and P. A. Lee, Phys. Rev. Lett. **76**, 1932 (1996).

[21] C. Janani, J. Merino, I. P. McCulloch, and B. J. Powell, Phys. Rev. Lett. **113**, 267204 (2014).

[22] H. L. Nourse, I. P. McCulloch, C. Janani, and B. J. Powell, Phys. Rev. B **94**, 214418 (2016).

[23] S. Reja and S. Nishimoto, Sci. Rep. **9**, 2691 (2019).

[24] A. Rüegg, J. Wen, and G. A. Fiete, Phys. Rev. B **81**, 205115 (2010).

[25] J. Wen, A. Rüegg, C. C. Joseph Wang, and G. A. Fiete, Phys. Rev. B **82**, 075125 (2010).

[26] M. Chen, H.-Y. Hui, S. Tewari, and V. W. Scarola, Phys. Rev. B **97**, 035114 (2018).

[27] M. F. López and J. Merino, Phys. Rev. B **100**, 075154 (2019).

[28] H. Yao, W.-F. Tsai, and S. A. Kivelson, Phys. Rev. B **76**, 161104(R) (2007).

[29] S. Sur, S.-S. Gong, K. Yang, and O. Vafek, Phys. Rev. B **98**, 125144 (2018).

[30] E. Dagotto, Rev. Mod. Phys. **85**, 849 (2013).

[31] Y. Yanagi and K. Ueda, Phys. Rev. B **90**, 085113 (2014).

[32] E. Khatami, R. R. P. Singh, W. E. Pickett, and R. T. Scalettar, Phys. Rev. Lett. **113**, 106402 (2014).

[33] C. Feng, H. Guo, and R. T. Scalettar, Phys. Rev. B **101**, 205103 (2020).

[34] H.-F. Lin, Y.-H. Chen, H.-D. Liu, H.-S. Tao, and W.-M. Liu, Phys. Rev. A **90**, 053627 (2014).

[35] J. Richter, J. Schulenburg, A. Honecker, and D. Schmalfuß, Phys. Rev. B **70**, 174454 (2004).

[36] G. Misguich and P. Sindzingre, J. Phys.: Condens. Matter **19**, 145202 (2007).

[37] B.-J. Yang, A. Paramekanti, and Y. B. Kim, Phys. Rev. B **81**, 134418 (2010).

[38] S. S. Jahromi and R. Orús, Phys. Rev. B **98**, 155108 (2018).

[39] A. Kitaev, Ann. Phys. **321**, 2 (2006).

[40] H. Yao and S. A. Kivelson, Phys. Rev. Lett. **99**, 247203 (2007).

[41] S. Dusuel, K. P. Schmidt, J. Vidal, and R. L. Zaffino, Phys. Rev. B **78**, 125102 (2008).

[42] A. L. Khosla, A. C. Jacko, J. Merino, and B. J. Powell, Phys. Rev. B **95**, 115109 (2017).

[43] B. J. Powell, J. Merino, A. L. Khosla, and A. C. Jacko, Phys. Rev. B **95**, 094432 (2017).

[44] Q. Si, R. Yu, and E. Abrahams, Nat. Rev. Mater. **1**, 16017 (2016).

[45] G. Kotliar and A. E. Ruckenstein, Phys. Rev. Lett. **57**, 1362 (1986).

[46] F. Lechermann, A. Georges, G. Kotliar, and O. Parcollet, Phys. Rev. B **76**, 155102 (2007).

[47] N. Lanatà, Y. Yao, C.-Z. Wang, K.-M. Ho, and G. Kotliar, Phys. Rev. X **5**, 011008 (2015).

[48] N. Lanatà, Y. Yao, X. Deng, V. Dobrosavljević, and G. Kotliar, Phys. Rev. Lett. **118**, 126401 (2017).

[49] See Supplemental Material at http://link.aps.org/supplemental/10.1103/PhysRevB.103.L081114, which includes Refs. [50–56], for technical details on RISB, the relation between the quasiparticle weight of the bands and the molecular orbitals, the explicit form of $\hat{H}$ in the dimer and trimer basis, and the magnetic phase diagram in the honeycomb-like regime.

[50] A. Isidori and M. Capone, Phys. Rev. B **80**, 115120 (2009).

[51] J. Bünemann, F. Gebhard, and R. Thul, Phys. Rev. B **67**, 075103 (2003).

[52] N. Lanatà, T.-H. Lee, Y.-X. Yao, and V. Dobrosavljević, Phys. Rev. B **96**, 195126 (2017).

[53] O. Parcollet, M. Ferrero, T. Ayral, H. Hafermann, I. Krivenko, L. Messio, and P. Seth, Comput. Phys. Commun. **196**, 398 (2015), version 1.4 .

[54] P. Seth, I. Krivenko, M. Ferrero, and O. Parcollet, Comput. Phys. Commun. **200**, 274 (2016).

[55] P. E. Blöchl, O. Jepsen, and O. K. Andersen, Phys. Rev. B **49**, 16223 (1994).

[56] I. Krivenko, ezARPACK—a C++ ARPACK-NG wrapper compatible with multiple matrix/vector algebra libraries: Release 0.9 (2020).

[57] J. Bünemann and F. Gebhard, Phys. Rev. B **76**, 193104 (2007).

[58] S. Burdin, A. Georges, and D. R. Grempel, Phys. Rev. Lett. **85**, 1048 (2000).

[59] L. Zhu, S. Kirchner, Q. Si, and A. Georges, Phys. Rev. Lett. **93**, 267201 (2004).

[60] F. Lechermann, Phys. Rev. Lett. **102**, 046403 (2009).

[61] F. Lu, J. Z. Zhao, H. Weng, Z. Fang, and X. Dai, Phys. Rev. Lett. **110**, 096401 (2013).
[62] A. Isidori, M. Berović, L. Fanfarillo, L. de' Medici, M. Fabrizio, and M. Capone, Phys. Rev. Lett. **122**, 186401 (2019).
[63] W. F. Brinkman and T. M. Rice, Phys. Rev. B **2**, 4302 (1970).
[64] J. Merino, B. J. Powell, and R. H. McKenzie, Phys. Rev. B **73**, 235107 (2006).
[65] T. Ohashi, N. Kawakami, and H. Tsunetsugu, Phys. Rev. Lett. **97**, 066401 (2006).
[66] C. Broholm, R. J. Cava, S. A. Kivelson, D. G. Nocera, M. R. Norman, and T. Senthil, Science **367**, eaay0668 (2020).
[67] K. Kanoda, Phys. C **282-287**, 299 (1997).
[68] R. H. McKenzie, arXiv:cond-mat/9802198.
[69] B. J. Powell and R. H. McKenzie, J. Phys.: Condens. Matter **18**, R827 (2006).
[70] A. C. Jacko, E. P. Kenny, and B. J. Powell, Phys. Rev. B **101**, 125110 (2020).
[71] C. Janani, J. Merino, I. P. McCulloch, and B. J. Powell, Phys. Rev. B **90**, 035120 (2014).
[72] A. Mattsson, P. Fröjdh, and T. Einarsson, Phys. Rev. B **49**, 3997 (1994).
[73] A. Banerjee, K. Damle, and A. Paramekanti, Phys. Rev. B **83**, 134419 (2011).
[74] S. Pujari, K. Damle, and F. Alet, Phys. Rev. Lett. **111**, 087203 (2013).
[75] M. S. Block, R. G. Melko, and R. K. Kaul, Phys. Rev. Lett. **111**, 137202 (2013).
[76] K. Harada, T. Suzuki, T. Okubo, H. Matsuo, J. Lou, H. Watanabe, S. Todo, and N. Kawashima, Phys. Rev. B **88**, 220408(R) (2013).
[77] S.-S. Gong, D. N. Sheng, O. I. Motrunich, and M. P. A. Fisher, Phys. Rev. B **88**, 165138 (2013).
[78] X.-L. Yu, D.-Y. Liu, P. Li, and L.-J. Zou, Phys. E **59**, 41 (2014).
[79] R. F. Bishop, P. H. Y. Li, O. Götze, J. Richter, and C. E. Campbell, Phys. Rev. B **92**, 224434 (2015).
[80] J. Merino, A. C. Jacko, A. L. Khosla, and B. J. Powell, Phys. Rev. B **94**, 205109 (2016).
[81] J. Merino, A. C. Jacko, A. L. Khosla, A. Ralko, and B. J. Powell, AIP Adv. **8**, 101430 (2018).
[82] J. Merino and A. Ralko, Phys. Rev. B **97**, 205112 (2018).
[83] S.-S. Gong, W. Zhu, and D. N. Sheng, Phys. Rev. B **92**, 195110 (2015).
[84] P. H. Y. Li, R. F. Bishop, and C. E. Campbell, J. Phys.: Conf. Ser. **702**, 012001 (2016).
[85] A. Mielke, J. Phys. A **24**, 3311 (1991).
[86] A. Mielke, J. Phys. A **25**, 4335 (1992).
[87] H. Tasaki, Phys. Rev. Lett. **69**, 1608 (1992).
[88] E. C. Stoner, J. Phys. Radium **12**, 372 (1951).
[89] B. J. Powell and R. H. McKenzie, Phys. Rev. Lett. **94**, 047004 (2005).
[90] B. J. Powell and R. H. McKenzie, Phys. Rev. Lett. **98**, 027005 (2007).
[91] S. Hoshino and P. Werner, Phys. Rev. Lett. **115**, 247001 (2015).
[92] S. Hoshino and P. Werner, Phys. Rev. B **93**, 155161 (2016).
[93] J. Merino, M. F. Lopez, and B. J. Powell, arXiv:2012.13211 [cond-mat.supr-con].